
AssembleNet: Searching for Multi-Stream Neural Connectivity in Video Architectures

Michael S. Ryoo, AJ Piergiovanni, Mingxing Tan, Anelia Angelova
 Google Brain
 mryoo@google.com

Abstract

Learning to represent videos is a very challenging task both algorithmically and computationally. Standard video CNN architectures have been designed by directly extending architectures devised for image understanding to a third dimension (using a limited number of space-time modules such as 3D convolutions) or by introducing a handcrafted two-stream design to capture both appearance and motion in videos. We interpret a video CNN as a collection of multi-stream space-time convolutional blocks connected to each other, and propose the approach of automatically finding neural architectures with better connectivity for video understanding. This is done by evolving a population of overly-connected architectures guided by connection weight learning. Architectures combining representations that abstract different input types (i.e., RGB and optical flow) at multiple temporal resolutions are searched for, allowing different types or sources of information to interact with each other. Our method, referred to as AssembleNet, outperforms prior approaches on public video datasets, in some cases by a great margin.

1 Introduction

Learning to represent videos is a challenging problem. Because of the property that a video is spatio-temporal data, its representation is required to abstract both appearance and motion information from the video. This is particularly so for understanding semantic contents in videos such as activity recognition. Previously, researchers approached this challenge by hand-designing a two-stream model taking two different types of inputs (e.g., RGB pixels and optical flow), obtaining successful results [20, 9, 7, 8, 6]. However, in most cases, combining appearance and motion information (i.e., the interactions between different streams) was done in a handcrafted way, e.g., by late fusion of outputs from individual modalities, without further exploration or optimization. Researchers confirmed that having a two-stream network design is beneficial, but the study on how or where different streams should interchange representations and what temporal aspect or resolution each stream or module should focus on has been very limited.

In this paper, we investigate how to learn feature representations across spatial and motion visual clues, a longstanding problem in video understanding. We propose a new neural architecture search algorithm with *connection learning guided evolution*, which focuses on finding higher-level connectivity between network blocks taking multiple types of inputs at different temporal resolutions. Each block itself is composed of multiple residual modules with (2+1)D convolutional layers, learning spatio-temporal representations. Our architecture evolution not only considers the connectivity between such multi-stream multi-resolution blocks, but also merges and splits network blocks to find better multi-stream video CNN architectures. Our objective is to address two main questions in video representation learning: (1) what feature representations do we need at each intermediate stage of the network at which resolution and (2) how such intermediate representations need to be combined/exchanged (i.e., connectivity). Unlike previous neural architecture search methods for images, which focus on finding a good module of convolutional layers to be repeated in

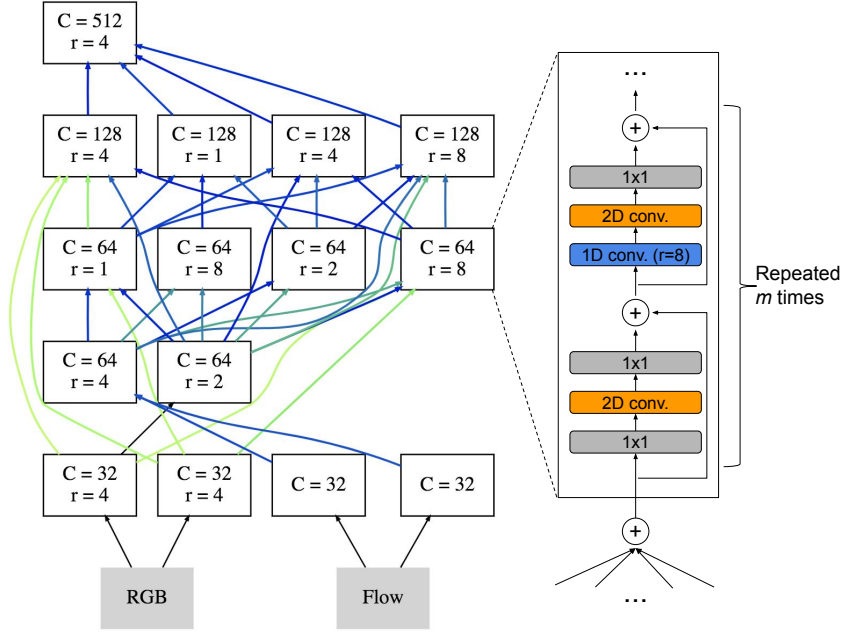


Figure 1: AssembleNet with multiple intermediate streams. Example learned architecture. Darker colors of connections indicate stronger connections. At each convolutional block, multiple 2D and (2+1)D residual modules are repeated alternatingly. Our network has 4 block levels (+ the stem level connected to raw data). Each convolutional block has its own output channel size (i.e., the number of filters) C and the temporal resolution r controlling the 1D temporal conv. layers in it.

a single-stream way [35, 17], our objective is to search for higher-level connections between multiple sequential/concurrent blocks to form multi-stream architectures. This is particularly necessary for video CNNs due to their inherent design handling multiple types of inputs and temporal resolutions.

We propose the concept of AssembleNet, a new method of fusing different sub-networks with different input modalities and temporal resolutions. We propose a general formulation that allows representing various forms of multi-stream CNNs as directed graphs, and present an efficient evolutionary algorithm to explore the network connectivity. Specifically, this is done by utilizing the learned connection weights to guide the evolution, in addition to randomly combining/splitting/connecting sub-network modules. We believe this is the first paper to (i) conduct research on automated architecture search with multi-stream connections for video understanding, and (ii) introduce the new connection-learning-guided evolutionary algorithm for neural architecture search. AssembleNet is a ‘family’ of learnable architectures; they provide a generic approach to learning interaction or feature representations across input modalities, which are (more importantly) optimized to the task at hand. Figure 1 shows an example AssembleNet. The proposed learned connectivity for video architectures is very effective as showcased with two very challenging benchmark datasets.

2 Previous work

A video is a spatio-temporal data (i.e., image frames concatenated along time axis), and its representation must abstract both spatial and temporal information in the video. Full 3D space-time (i.e., XYT) convolutional layers as well as (2+1)D convolutional layers have been popularly used to represent videos [22, 3, 23, 30]. Researchers studied replacing 2D convolutional layers in standard image-based CNNs such as Inception [21] and ResNet [11], so that it can be directly used for video classification.

Using two-stream network designs has also been extremely popular in video CNNs [20, 7–9]. The two-stream architecture allows a model to efficiently capture both motion and appearance in videos. The idea is to train and maintain two different CNN models each responsible for abstracting RGB appearance information and explicit optical flow-based motion information, then fuse the CNNs for the final video representation. In addition, a recent study [6] confirmed that learning two model streams with different temporal resolutions (e.g., 24 vs. 3 frames per second) and having intermediate

connections to combine them benefits video classification, even when only using RGB frames as an input. Late fusion of the two-stream representations, as well as architectures with more intermediate connections [5], have been designed. However, these video CNN architectures were the results of careful manual designs by human experts.

Neural Architecture Search (NAS), the concept of automatically finding better CNN architectures based on data, is becoming increasingly popular [34, 35, 14]. Rather than relying on human expert knowledge to design a CNN model, neural architecture search allows the machines to generate better performing CNN models optimized for the data. Use of reinforcement learning [34, 35] controllers as well as evolutionary algorithms [17] has been studied, and they meaningfully outperform handcrafted architectures. Most of these works focus on learning architectures of ‘modules’ (i.e., groupings of layers and their connections) to be repeated within a fixed single-stream meta-architecture (e.g., ResNet taking RGB) for image-based object classification. One-shot architecture search [2, 15] learning differentiable connections has also been studied. However, similar to other NAS works, it focused on module-level architecture search. Furthermore, it is very challenging to directly extend such work for the multi-stream search for videos, as it requires preparing all possible layers the final architecture may consider using. In multi-stream video CNNs, there are many possible convolutional blocks with different resolutions, and fully connecting them requires a significant amount of memory and training data, which makes it infeasible. Ahmed and Torresani [1] used learnable gating to connect multiple residual module branches, which similarly requires training of all possible modules and connections.

Our work is also related to the recent RandWire network [29], which showed that randomly connecting a sufficient number of convolutional layers creates architectures with high performance. However, similar to the previous NAS works, it focused only on generating connections between the conv. layers within a block. The meta-architecture was fixed as a single stream model taking a single input modality (i.e., an image). On the other hand, in this work, our objective is to learn high-level connectivity between multi-stream blocks for video understanding. We experimentally confirm that in our multi-stream video CNN case where multiple types of input modalities need to be considered at various resolutions, randomly connecting blocks is insufficient and an (intelligent) evolutionary strategy is necessary.

3 AssembleNet

We propose a new principled way to find better neural architectures for video representation learning. We first expand a video CNN to a multi-resolution, multi-stream model composed of multiple sequential and concurrent neural blocks, and introduce a novel algorithm to search for the optimal connectivity between the blocks for a given task.

We model a video CNN architecture as a collection of convolutional blocks (i.e., sub-networks) connected to each other. Each block is composed of a residual module of space-time convolutional layers repeated multiple times, while having its own temporal resolution. The objective of our video architecture search is to automatically (1) decide the number of parallel blocks (i.e., how many streams to have) at each level of the network, (2) choose their temporal resolutions, and (3) find the optimal connectivity between such multi-stream neural blocks across various levels. The highly interconnected convolutional blocks allow learning of the video representation combining multiple input modalities at various temporal resolutions. We introduce the concept of connection-learning-guided architecture evolution to enable the multi-stream architecture search.

We name our final architecture as an ‘AssembleNet’, since it is formulated by assembling (i.e., merging, splitting, and connecting) multiple building blocks.

3.1 Graph formulation

In order to make our neural architecture evolution consider multiple different streams with different modalities at different temporal resolutions, we formulate the multi-stream model as a directed acyclic graph. Each node in the graph corresponds to a sub-network composed of multiple convolutional layers (i.e., a block), and the edges specify the connections between such sub-networks. Each architecture is denoted as $G_i = (N_i, E_i)$ where $N_i = \{n_{0i}, n_{1i}, n_{2i}, \dots\}$ is the set of nodes and E_i is the set of edges defining their connectivity.

Nodes. A node in our graph representation is a ResNet block composed of a fixed number of interleaved 2D and (2+1)D residual modules. A ‘2D module’ is composed of a 1x1 conv. layer, one 2D conv. layer with filter size 3x3, and one 1x1 convolutional layer. A ‘(2+1)D module’ consists of a temporal 1D convolutional layer (with filter size 3), a regular 2D conv. layer, and a 1x1 conv. layer. In each block, we repeat a regular 2D residual module followed by the (2+1)D residual module m number of times.

Each node has its own block level, which naturally decides the directions of the edges connected to it. Similar to the standard ResNet models, we made the nodes have a total of four block levels (+ the stem level). Having multiple nodes of the same level means the architecture has multiple parallel ‘streams’. Figure 1 illustrates an example. Each level has a different m value: 1.5, 2, 3, and 1.5. $m = 1.5$ means that there is one 2D module, one (2+1)D module, and one more 2D module. That is, the depth of our network is 50 conv. layers. We also have a batch normalization layer followed by a ReLU after every conv. layer.

There are two special types of nodes with different layer configurations: source nodes and sink nodes. A source node in the graph directly takes the input and applies a small number of convolutional/pooling layers (it is often referred as the ‘stem’ of a CNN model). In video CNNs, the input is a 4D tensor (XYT + channel) obtained by concatenating either RGB frames or optical flow images along the time axis. Source nodes are treated as level-0 nodes. The source node is composed of one 2D conv. layer of size 7x7, one 1D temporal conv. layer of size 5, and one spatial max pooling layer. The 1D conv. is omitted in optical flow stems. A sink node generates the final output of the model, and it is composed of one pooling, one fully connected, and one softmax layer. The sink node is also responsible for combining of the outputs of multiple nodes at the highest level, by concatenating them after the pooling. More details are provided in Appendix.

Each node in the graph also has two attributes controlling the convolutional block: its temporal resolution and the number of channels. We use temporally dilated 1D convolution to dynamically change the resolution of the temporal convolutional layers in different blocks, which are discussed more below. The channel size (i.e., the number of filters) of a node could take arbitrary values, but we constrain the sum of the channels of all nodes in the same block level to be a constant.

Temporally Dilated 1D Convolution. One of the objectives is to allow the video architectures to look at multiple possible temporal resolutions. This could be done by preparing actual videos with different temporal resolutions as in [6] or by using temporally ‘dilated’ convolutions as we introduce here. Having dilated filters allow temporal 1D conv. layers to focus on different temporal resolution without losing temporal granularity. This essentially is a 1D temporal version of standard 2D dilated convolutions used in [4] or [31]:

Let k be a temporal filter (i.e., a vector) with size $2d + 1$. The dilated convolution operator $*_r$ is similar to the regular convolution but has different steps for the summation, described as:

$$(F *_r k)(t) = \sum_{t_1 + rt_2 = t} F(t_1)k(t_2 + d) \quad (1)$$

where t , t_1 , and t_2 are time indexes. r indicates the temporal resolution (or the amount of dilation), and the standard 1D temporal convolution is a special case where $r = 1$. In the actual implementation, this is done by inserting $r - 1$ number of zeros between each element of k to generate k' , and then convolving such zero-inflated filters with the input: $F *_r k = F * k'$. Importantly, the use of the dilated convolution allows different intermediate sub-network blocks (i.e., not just input stems) to focus on very different temporal resolutions at different levels of the convolutional architecture.

Note that our temporally dilated convolution is different from the one used in [13], which designed a specific layer to combine representations from different frames with various step sizes. Our layers dilate the temporal filters themselves. Our dilated convolution can be viewed as a direct temporal version of the standard dilated convolutions used in [4, 31].

Edges. Each directed edge specifies the connection between two sub-network blocks, and it describes how a representation is transferred from one block to another block. We constrain the direction of each edge so that it is connected from a lower level block to a higher level block to avoid forming a cycle and allow parallel streams. A node may receive inputs from any number of lower-level nodes (including skip connections) and provide its output to any number of higher-level nodes.

Our architectures use a (learnable) weighted summation to aggregate inputs given from multiple connected nodes. That is, an input to a node is computed as $F^{in} = \sum_i \text{sigmoid}(w_i) \cdot F_i^{out}$, where

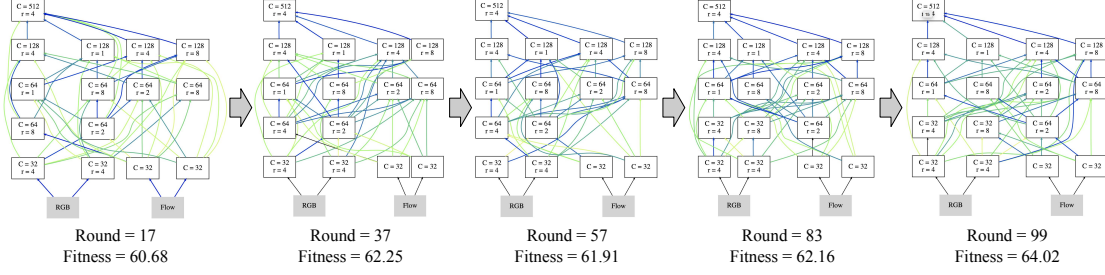


Figure 2: An example showing a sequence of architecture evolution. These architectures have an actual parent-child relationships. The fitness of the third model was worse than the second model (due to random mutations), but it was high enough to survive in the population pool and eventually evolve to a better model.

F_i^{out} are output tensors (i.e., representations) of the nodes connected to the node and w_i are their corresponding weights. Importantly, each w_i is considered as a variable that has to be learned from training data through back propagation. This has two key advantages compared to conventional feature map concatenation: (i) It is able to maintain the input tensor size to be consistent regardless of the number of connections. (ii) We use learned connection weights to ‘guide’ our architecture evolution algorithm in a preferable way, which we discuss more in Section 3.2.

If the inputs from different nodes differ in their spatial size, we add spatial max pooling and striding to match their spatial size. If the inputs have different channel sizes, we add a 1×1 conv. layer to match the bigger channel size. Temporal sizes of the representations is always consistent in our graphs, as there is no temporal striding in our formulation and the layers in the nodes are fully convolutional.

3.2 Evolution

We design an evolutionary algorithm with discrete mutation operators that modify nodes and edges in architectures over iterations. The algorithm maintains a population of P different architectures, $P = \{G_1, G_2, \dots, G_{|P|}\}$, where each architecture G is represented with a set of nodes and their edges as described above.

The initial population is formed by preparing a fixed number of randomly connected architectures (e.g., $|P| = 20$). Specifically, we (1) prepare a fixed number of stems and nodes at each level (e.g., two per level), (2) apply a number of node split/merge mutation operators which we discuss more below, and (3) randomly connect nodes with the probability $p = 0.5$ while discarding architectures with graph depth < 4 . As mentioned above, edges are constrained so that there is no directed edge reversing the level ordering. Essentially, a set of overly-connected architectures are used as a starting point. Temporal resolutions are randomly assigned to the nodes.

We use the tournament selection algorithm [10] as the main evolution framework: At each evolution round, the algorithm updates the population by selecting a ‘parent’ architecture and mutating (i.e., modifying) it to generate a new ‘child’ architecture. The parent is selected by randomly sampling a subset of the entire population $P' \subset P$, and then computing the architecture with the highest ‘fitness’: $G_p = \arg\max_{G_i \in P'} f(G_i)$ where $f(G)$ is the fitness function. Our fitness is defined as a video classification accuracy of the model, measured by training the model with a certain number of initial iterations and then evaluating on the validation set. More specifically, we use top-1 accuracy + top-5 accuracy as the fitness function. The child is added into the population, and the model with the least fitness is discarded from the population.

A child is evolved from the parent by applying a random number of mutation operators. The mutation operators include (1) a random modification of the temporal resolution of a convolutional block (i.e., a node) as well as (2) a merge or split of a block. Importantly, we also introduce a new mutation operator to implement the connection-learning-guided evolution, which (3) modifies the block connectivity (i.e., edges) based on their learned weights. When splitting a node into two nodes, we make their input/output connections identical while making the number of channels in their convolutional layers half that of the node before the split (i.e., $C = C_p/2$ where C_p is the channel size of the parent). More details are found in Appendix. As a result, we maintain the total number of parameters; splitting/merging does not change the number of parameters of the convolutional blocks.

Connection-learning-guided mutation. Instead of randomly adding, removing or modifying block connections to generate the child architecture, we take advantage of the learned connection weights from its parent architecture. Let E_p be the set of edges of the parent architecture. Then the edges of the child architecture E_c are inherited from E_p , by only maintaining high-weight connections while replacing the low-weight connections. Specifically, $E_c = E_c^1 \cup E_c^2$:

$$E_c^1 = \{e \in E_p \mid W_e > B\}, \quad E_c^2 = \left\{ e \in (E_* - E_p) \mid \frac{|E_p - E_c^1|}{|E - E_p|} > X \right\} \quad (2)$$

where $X \sim \text{unif}(0, 1)$ and E_* is the set of all possible edges. E_c^1 corresponds to the edges the child architecture inherits from the parent architecture, decided based on the learned weight of the edge W_e . This is possible because the fitness function involves learning parameters of each architecture including the connection weights when they are generated. B , which controls whether or not to keep an edge from the parent architecture, could either be a constant threshold or a random variable following a uniform distribution: $B = b$ or $B = X_B \sim \text{unif}(0, 1)$. E_c^2 corresponds to the edges randomly added which were not in the parent architecture. We enumerate through each possible new edge, and randomly add it with the probability of $|E_p - E_c^1|/|E - E_p|$. This makes the expected total number of added edges to be $|E_p - E_c^1|$, maintaining the size of E_c .

Figure 2 shows an example of the evolution process.

4 Experiments

4.1 Implementation details

Initial architectures are formed by randomly preparing either $\{2 \text{ or } 4\}$ stems, two nodes per level at levels 1~3, and one node at level 4. The initial channel sizes are 64 for level 1 nodes, 128 for level 2, 256 for level 3, and 512 for level 4. We then apply 1~5 number of node split operators so that each architecture has a different number of nodes. Splitting a node makes the resulting nodes have 1/2 output channels. Each node is initialized with a random temporal resolution, where we consider the temporal resolution of 1, 2, 4, and 8. As mentioned, each possible connection is then added with the probability of $p = 0.5$.

At each evolution round, the best-performing parent architecture is selected from a random subset of the population with its size=5 (the population size is 20). The child architecture is generated by inheriting/modifying the connections from the parent architecture as described in Section 3.2. 0~4 random number of node split, merge, or temporal resolution change mutation operators were then applied. Evaluation of each architecture (i.e., measuring the fitness) is done by applying 10K training iterations (batch size = 512) and then measuring its top-1 + top-5 accuracy on the validation subset. The evolution was continued for ~200 rounds, although a good performing architecture was found within only 40 rounds (e.g., Figure 3-right). Figure 1 shows the model found at the 101st round. 10K training iterations of each model during evolution took 3~5 hours; with our setting, evolving a model for 40 rounds took less than a day.

Once the architecture is found, we prune the edges with low weights to make it more compact, and fully trained it with 50K iterations. The final training of AssembleNet takes ~24 hours.

4.2 Datasets

Moments in Time (MiT) Dataset The Moments in Time (MiT) dataset [16] is a large-scale video classification dataset with more than 800K videos (~3 seconds per video). It is a very challenging dataset with the state-of-the-art models obtaining less than 30% accuracy. We use this dataset for the architecture evolution, and train/test the evolved models. We chose the MiT dataset because it provides a sufficient amount of training data for video CNN models and allows stable comparison against previous models. For instance, another large-scale video dataset, Kinetics [3], is not a static dataset. It has lost about 10~20% of the videos since its launch. It is thus difficult to compare against previously reported numbers due to missing training and test data. The MiT dataset does not suffer from this problem. We used its standard classification evaluation setting.

Charades Dataset We further test on the popular Charades dataset [19] which is unique in the activity recognition domain as it contains long sequences. It is one of the largest public datasets with continuous action videos, containing 9858 videos of 157 classes (7990 training and 1868 testing

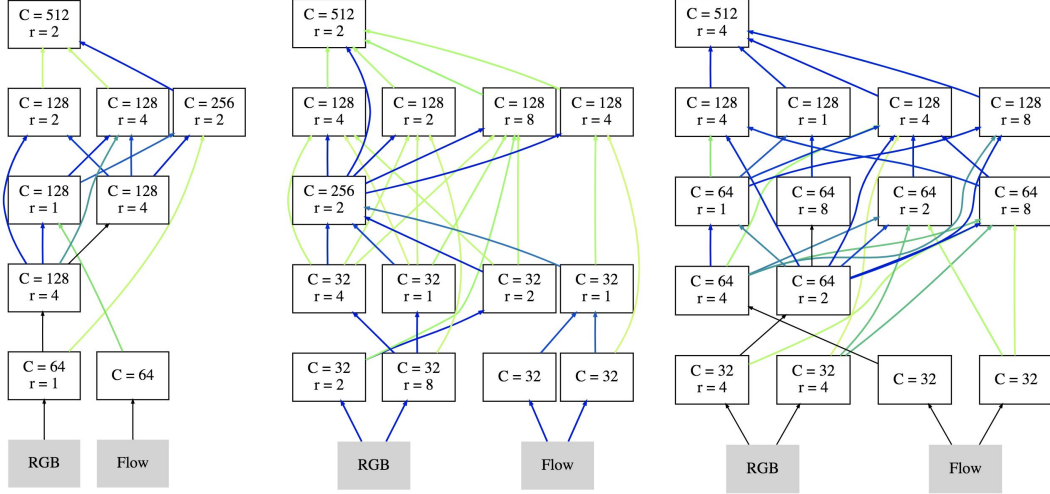


Figure 3: More AssembleNet examples. Similarly good performing diverse architectures, all with higher-than-50% accuracy on Charades. Darker edges mean higher weights.

Table 1: State-of-the-art action classification performances on Charades [19].

Method	modality	mAP
2-Strm. [20] (from [18])	RGB+Flow	18.6
Asyn-TF [18]	RGB+Flow	22.4
CoViAR [28]	Compressed	21.9
MultiScale TRN [33]	RGB	25.2
I3D [3]	RGB	32.9
I3D [3] (from [25])	RGB	35.5
I3D-NL [25]	RGB	37.5
STRG [26]	RGB	39.7
LFB [27]	RGB	42.5
SlowFast [6]	RGB+RGB	45.2
Two-stream (2+1)D ResNet	RGB+Flow	46.5
AssembleNet	RGB+Flow	51.6

Table 2: State-of-the-art action classification accuracies on Moments in Time [16].

Method	modality	Top-1	Top-5
ResNet50-ImageNet	RGB	27.16	51.68
TSN [24]	RGB	24.11	49.10
BNInception-Flow [12]	Flow	11.60	27.40
TSN-Flow [24]	Flow	15.71	34.65
TSN-2Stream [24]	RGB+Flow	25.32	50.10
TRN-Multiscale [33]	RGB+Flow	28.27	53.87
Two-stream (2+1)D	RGB+Flow	28.54	55.54
I3D [3]	RGB+Flow	29.51	56.06
AssembleNet	RGB+Flow	31.02	57.38

videos). It is a challenging dataset due to the duration and variety of the activities. Activities may temporally overlap in a Charades video, requiring the model to predict multiple class labels per video. We used the standard ‘Charades_v1_classify’ setting for the evaluation.

4.3 Results

The architecture search is done on the MiT dataset, and then the found models are trained and tested on the Charades and MiT datasets. For Charades training, the models were pre-trained with MiT. Tables 1 and 2 compare the performance of AssembleNet against the state-of-the-art models. AssembleNet is outperforming the prior works in both datasets, setting the new state-of-the-art results for them. Its performance on MiT is the first above 31% (with all previous in the tens and twenties). We also note that the performances on Charades is even more impressive at 51.6 whereas previous known results are 42.5 and 45.2 (arXiv report).

In addition, we compare the proposed connection-learning-guided evolution with the random architecture search and the standard evolutionary algorithm with random connection mutations. The standard evolutionary algorithm is able to modify a similar number of each architecture’s total connections (which is 1/3 of connections), as that is roughly the number of edges the connection-learning-guided evolution modifies. Figure 4 shows the results. We observe that the connection-learning-guided evolution is able to find better architectures, and it is also able to do that more quickly. The standard evolution performs similarly to random search and is not as effective. We believe this is due to the

Table 3: Comparison between the evolved AssembleNet and multiple network architectures. All these models are with the connection weight learning. Four-stream architectures are reported in this paper for the first time, and are generally very effective.

Architecture	MiT	Charades
Two-stream (late fusion)	28.54	46.5
Two-stream (fusion at lv. 4)	30.0	47.7
Two-stream (fully, fuse at 4)	29.87	46.0
Four-stream (fully, fuse at 4)	29.98	48.8
Random	29.77	47.4
AssembleNet (2-stem version)	30.75	50.2
AssembleNet	31.02	51.6

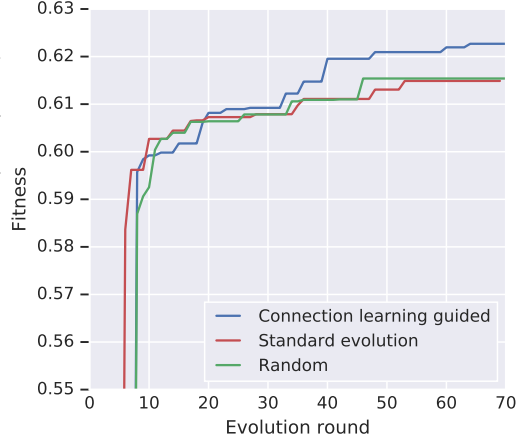


Figure 4: Comparison of different search methods. Y-axis corresponds to the average fitness score of the three top-performing models in each pool.

large search space the approach is required to handle, which is exponential to the number of possible connections. For instance, if there are N nodes, the search space complexity is $2^{O(N^2)}$ just for the connectivity search. Note that the initial ~ 30 rounds are always used for random initialization of the model population, regardless of the search method.

4.4 Ablation study

We conduct an ablation study comparing the evolved AssembleNet to multiple (2+1)D two-stream (or multi-stream) architectures which are designed to match the abilities of AssembleNet but without evolution. We note that these include strong architectures that has not been explored before, such as the four-stream model with dense intermediate connectivity. We design competitive networks having various connections between streams, where the connection weights are also learned (see the supplementary material for detailed descriptions and visualizations). Table 3 shows the results, demonstrating that these architectures with learnable inter-connectivity are very powerful themselves and evolution is further beneficial. We also evaluated an architecture with connectivity only from the flow stream to RGB, inspired by [9, 6] for the MiT dataset which gave 30.2% accuracy (which is not as accurate as AssembleNet). Randomly generated models (from 50 rounds of random search) are also evaluated, confirming that not all architectures perform equally well.

4.5 General findings

As the result of connection-learning-guided architecture evolution, non-obvious and non-intuitive connections are found (Figure 3). As expected, more than one possible “connectivity” solution can yield similarly good results. Simultaneously, models with random connectivity performed poorly compared to the found AssembleNet. The observations also include: (1) The models preferred to have only one block at the highest level. Although we allowed the search to consider having more than one block at level 4, it always ended up using only one block. (2) The final block preferred simple connections gathering all outputs of the blocks in the 2nd last level. (3) Naturally, many models used multiple blocks with different temporal resolutions at the same level, justifying the necessity of the multi-stream architectures. (4) Often, there were 1 or 2 blocks heavily connected to many other blocks. (5) Architectures preferred using more than 2 streams, usually using 4 at many levels.

5 Conclusion

We present a new approach for neural architecture search using connection-learning-guided architecture evolution. The goal is to find multi-stream architectures with better connectivity (and temporal resolutions) for video representation learning. Our experiments confirm that the evolved models outperform previous models on two challenging benchmarks, establishing a new state-of-the-art.

References

- [1] K. Ahmed and L. Torresani. Connectivity learning in multi-branch networks. In *Workshop on Meta-Learning (MetaLearn), NeurIPS*, 2017.
- [2] G. Bender, P.-J. Kindermans, B. Zoph, V. Vasudevan, and Q. Le. Understanding and simplifying one-shot architecture search. In *International Conference on Machine Learning (ICML)*, 2018.
- [3] J. Carreira and A. Zisserman. Quo vadis, action recognition? a new model and the kinetics dataset. In *Proceedings of the IEEE Conference on Computer Vision and Pattern Recognition (CVPR)*, 2017.
- [4] L.-C. Chen, G. Papandreou, I. Kokkinos, K. Murphy, and A. L. Yuille. Deeplab: Semantic image segmentation with deep convolutional nets, atrous convolution, and fully connected crfs. *IEEE TPAMI*, 40(4), 2018.
- [5] A. Diba, M. Fayyaz, V. Sharma, M. Paluri, J. Gall, R. Stiefelhagen, and L. V. Gool. Holistic large scale video understanding. In *CoRR:1904.11451*, 2019.
- [6] C. Feichtenhofer, H. Fan, J. Malik, and K. He. Slowfast networks for video recognition. *arXiv preprint arXiv:1812.03982*, 2018.
- [7] C. Feichtenhofer, A. Pinz, and R. Wildes. Spatiotemporal residual networks for video action recognition. In *Advances in Neural Information Processing Systems (NeurIPS)*, pages 3468–3476, 2016.
- [8] C. Feichtenhofer, A. Pinz, and R. P. Wildes. Spatiotemporal multiplier networks for video action recognition. In *Proceedings of the IEEE Conference on Computer Vision and Pattern Recognition (CVPR)*, pages 4768–4777, 2017.
- [9] C. Feichtenhofer, A. Pinz, and A. Zisserman. Convolutional two-stream network fusion for video action recognition. In *Proceedings of the IEEE Conference on Computer Vision and Pattern Recognition (CVPR)*, pages 1933–1941, 2016.
- [10] D. E. Goldberg and K. Deb. A comparative analysis of selection schemes used in genetic algorithms. In *Foundations of Genetic Algorithms*, pages 69–93. Morgan Kaufmann, 1991.
- [11] K. He, X. Zhang, S. Ren, and J. Sun. Deep residual learning for image recognition. In *Proceedings of the IEEE Conference on Computer Vision and Pattern Recognition (CVPR)*, 2016.
- [12] S. Ioffe and C. Szegedy. Batch normalization: Accelerating deep network training by reducing internal covariate shift. In *International Conference on Machine Learning (ICML)*, 2015.
- [13] C. Lea, M. D. Flynn, R. Vidal, A. Reiter, and G. D. Hager. Temporal convolutional networks for action segmentation and detection. In *Proceedings of the IEEE Conference on Computer Vision and Pattern Recognition (CVPR)*, 2017.
- [14] C. Liu, B. Zoph, M. Neumann, J. Shlens, W. Hua, L.-J. Li, L. Fei-Fei, A. Yuille, J. Huang, and K. Murphy. Progressive neural architecture search. In *Proceedings of European Conference on Computer Vision (ECCV)*, 2018.
- [15] H. Liu, K. Simonyan, and Y. Yang. DARTS: Differentiable architecture search. In *International Conference on Learning Representations*, 2019.
- [16] M. Monfort, A. Andonian, B. Zhou, K. Ramakrishnan, S. A. Bargal, T. Yan, L. Brown, Q. Fan, D. Gutfrund, C. Vondrick, et al. Moments in time dataset: one million videos for event understanding. *arXiv preprint arXiv:1801.03150*, 2018.
- [17] E. Real, A. Aggarwal, Y. Huang, and Q. V. Le. Regularized evolution for image classifier architecture search. In *Proceedings of AAAI Conference on Artificial Intelligence (AAAI)*, 2019.
- [18] G. A. Sigurdsson, S. Divvala, A. Farhadi, and A. Gupta. Asynchronous temporal fields for action recognition. In *Proceedings of the IEEE Conference on Computer Vision and Pattern Recognition (CVPR)*, 2017.
- [19] G. A. Sigurdsson, A. Gupta, C. Schmid, A. Farhadi, and K. Alahari. Charades-ego: A large-scale dataset of paired third and first person videos. *arXiv preprint arXiv:1804.09626*, 2018.
- [20] K. Simonyan and A. Zisserman. Two-stream convolutional networks for action recognition in videos. In *Advances in Neural Information Processing Systems (NeurIPS)*, pages 568–576, 2014.

- [21] C. Szegedy, V. Vanhoucke, S. Ioffe, J. Shlens, and Z. Wojna. Rethinking the inception architecture for computer vision. In *Proceedings of the IEEE Conference on Computer Vision and Pattern Recognition (CVPR)*, pages 2818–2826, 2016.
- [22] D. Tran, L. D. Bourdev, R. Fergus, L. Torresani, and M. Paluri. C3d: generic features for video analysis. *CoRR, abs/1412.0767*, 2(7):8, 2014.
- [23] D. Tran, H. Wang, L. Torresani, J. Ray, Y. LeCun, and M. Paluri. A closer look at spatiotemporal convolutions for action recognition. In *Proceedings of the IEEE Conference on Computer Vision and Pattern Recognition (CVPR)*, pages 6450–6459, 2018.
- [24] L. Wang, Y. Xiong, Z. Wang, Y. Qiao, D. Lin, X. Tang, and L. Van Gool. Temporal segment networks: Towards good practices for deep action recognition. In *Proceedings of European Conference on Computer Vision (ECCV)*, pages 20–36. Springer, 2016.
- [25] X. Wang, R. Girshick, A. Gupta, and K. He. Non-local neural networks. In *Proceedings of the IEEE Conference on Computer Vision and Pattern Recognition (CVPR)*, pages 7794–7803, 2018.
- [26] X. Wang and A. Gupta. Videos as space-time region graphs. In *Proceedings of European Conference on Computer Vision (ECCV)*, pages 399–417, 2018.
- [27] C.-Y. Wu, C. Feichtenhofer, H. Fan, K. He, P. Krähenbühl, and R. Girshick. Long-term feature banks for detailed video understanding. *arXiv preprint arXiv:1812.05038*, 2018.
- [28] C.-Y. Wu, M. Zaheer, H. Hu, R. Manmatha, A. J. Smola, and P. Krähenbühl. Compressed video action recognition. In *Proceedings of the IEEE Conference on Computer Vision and Pattern Recognition (CVPR)*, pages 6026–6035, 2018.
- [29] S. Xie, A. Kirillov, R. Girshick, and K. He. Exploring randomly wired neural networks for image recognition. In *CoRR:1904.01569*, 2019.
- [30] S. Xie, C. Sun, J. Huang, Z. Tu, and K. Murphy. Rethinking spatiotemporal feature learning: Speed-accuracy trade-offs in video classification. In *Proceedings of European Conference on Computer Vision (ECCV)*, pages 305–321, 2018.
- [31] F. Yu and V. Koltun. Multi-scale context aggregation by dilated convolutions. In *International Conference on Learning Representations*, 2016.
- [32] C. Zach, T. Pock, and H. Bischof. A duality based approach for realtime tv-l 1 optical flow. In *Joint Pattern Recognition Symposium*, pages 214–223. Springer, 2007.
- [33] B. Zhou, A. Andonian, A. Oliva, and A. Torralba. Temporal relational reasoning in videos. In *Proceedings of European Conference on Computer Vision (ECCV)*, pages 803–818, 2018.
- [34] B. Zoph and Q. Le. Neural architecture search with reinforcement learning. In *International Conference on Learning Representations*, 2017.
- [35] B. Zoph, V. Vasudevan, J. Shlens, and Q. V. Le. Learning transferable architectures for scalable image recognition. In *Proceedings of the IEEE Conference on Computer Vision and Pattern Recognition (CVPR)*, 2018.

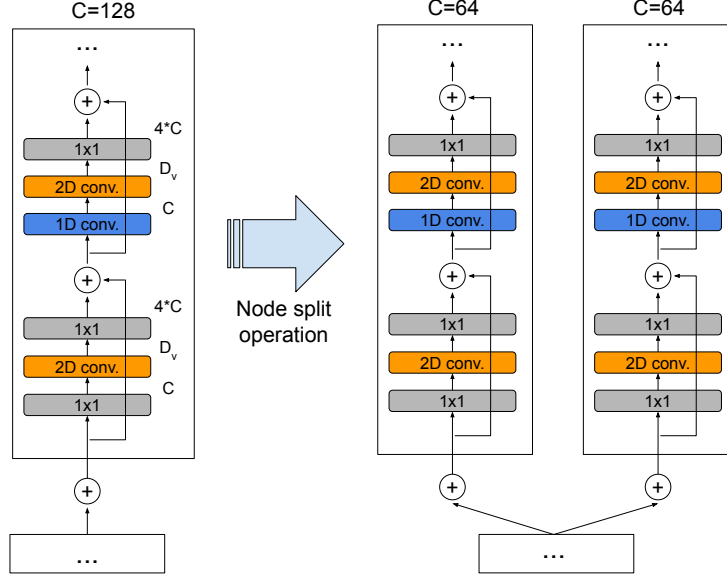


Figure 5: An illustration of the node split mutation operator, used for both evolution and initial architecture population generation.

A Appendix

A.1 Channel sizes of the layers and node split/merge mutations

As we described in the main paper, each node (i.e., a convolutional block) has a parameter C controlling the number of filters of the convolutional layers in the block. When splitting or merging blocks, the number of filters are split or combined respectively. Figure 5 provides a visualization of a block with number of filter specified to the right and a split operation. While many designs are possible, we design the blocks and splitting as follows. The size of 1x1 convolutional layers and 1D temporal convolutional layers are strictly governed by C , having the channel size of C (some $4C$). On the other hand, the number of 2D convolutional layer is fixed per level as a constant D_v where v is the level of the block. $D_1 = 64$, $D_2 = 128$, $D_3 = 256$, and $D_4 = 512$. The layers in the stems have 64 channels if there are only two stems and 32 if there are four stems.

When a node is split into two nodes, we update the resulting two nodes' channel sizes to be half of their original node. This enables us to maintain the total number of model parameters before and after the node split to be identical. The first 1x1 convolutional layer will have half the parameters after the split, since its output channel size is now 1/2. The 2D convolutional layer will also have exactly half the parameters, since its input channel size is 1/2 while the output channel size is staying fixed. The next 1x1 convolutional layer will have the fixed input channel size while the output channel size becomes 1/2: thus the total number of parameters would be 1/2 of the original parameters. Merging is done with the opposite operation, similarly preserving the total number of parameters.

A.2 Hand-designed models used in ablation study

Figure 6 illustrates the actual architectures of the hand-designed (2+1)D CNN models used in our ablation study. We also show the final learned weights of the connections, illustrating which connections the model ended up using or not using. We note that these architectures are also very enlightening as the connectivity within them are learned in the process. We observe that stronger connections tend to be formed later for 2-stream architectures. For 4-stream architectures, stronger connections do form early, and, not surprisingly, a connection to at least one node of a different modality is established, i.e. a node stemming from RGB will connect to at least one flow node at the next level and vice versa.

Below is a more detailed description of the networks used in the main paper: "Two-stream (late fusion)" means that the model has two separate streams at every level including the level 4, and

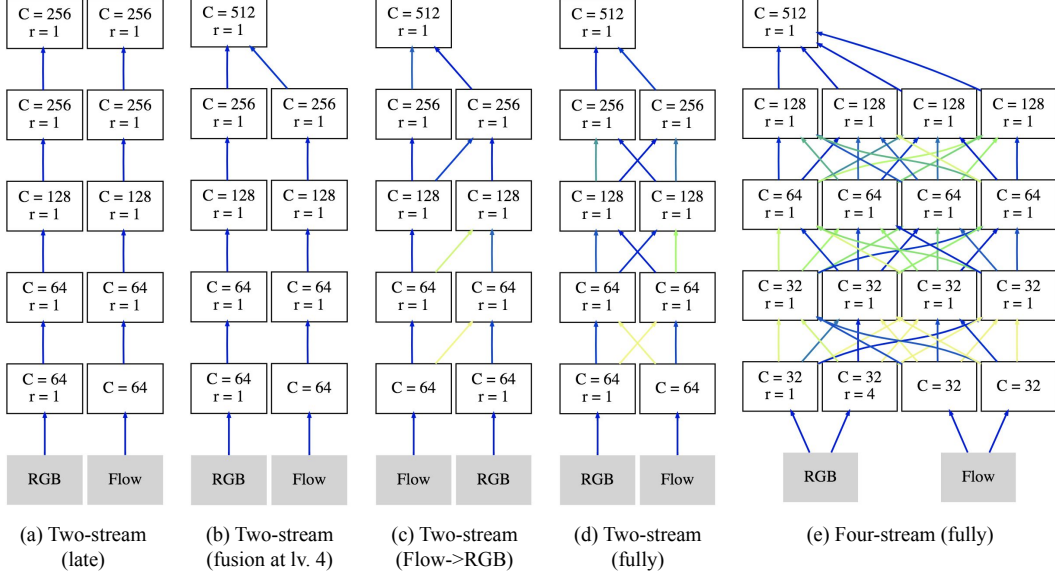


Figure 6: Illustration of hand-designed baseline (2+1)D CNN models used in our ablation study.

the outputs of such two level 4 nodes are combined for the final classification. “Fusion at lv. 4” is the model that only has one level 4 node to combine the outputs of the two level 3 nodes using a weighted summation. “Two-stream (fully)” means that the model has two nodes at each level 1-3 and one node at level 4, and each node is always connected to every node in the immediate next level. “Flow->RGB” means that only the RGB stream nodes combine outputs from both RGB and flow stream nodes of the immediate lower level.

A.3 AssembleNet model/layer details

We also provide the final AssembleNet model in table form in Table 4. In particular, the 2nd element of each block description shows the list of where the input to that block is coming from (i.e., the connections). As mentioned in the main paper, 2D and (2+1)D residual modules are repeated in each block. The number of repetitions m are 1.5, 2, 3, and 1.5 at each level. $m = 1.5$ means that we have one 2D residual module, one (2+1)D module, and one more 2D module. This makes the number of convolutional layers of each block at levels 1-4 to be 9, 12, 18, and 9. In addition, a stem has at most 2 convolutional layers. The total depth of our network is 50, similar to a conventional (2+1)D ResNet-50.

If a block has a spatial stride of 2, the striding happens at the first 2D convolutional layer of the block. In the stem which has the spatial stride of 4, the striding of size 2 happens twice, once at the 2D convolutional layer and at the max pooling layer. As suggested in the main paper, the model has a batch normalization layer followed by ReLU after every convolutional layer regardless of its type (i.e., 2D, 1D, and 1x1). 2D conv. filter sizes are 3x3, and 1D conv. filter sizes are 3.

A.4 Sink node details

When each evolved or baseline (2+1)D model is applied to a video, it generates a 5D (BTYXC) tensor after the final convolutional layer, where B is the size of the batch and C is the number of channels. The sink node is responsible for mapping this into the output vector, whose dimensionality is identical to the number of video classes in the dataset. The sink node first applies a spatial average pooling to generate a 3D (BTC) tensor. If there are multiple level 4 nodes (which rarely is the case), the sink node combines them into a single tensor by averaging/concatenating them. Averaging or concatenating does not make much difference empirically. Next, temporal average pooling is applied to make the representation a 2D (BC) tensor, and the final fully connected layer and the soft max layer is applied to generate the final output.

Table 4: The table form of the AssembleNet model with detailed parameters. This model corresponds to Figure 1 of the main paper. The parameters correspond to {node_level, input_node_list, C , r , and spatial stride}

Index	Block parameters
0	0, [RGB], 32, 4, 4
1	0, [RGB], 32, 4, 4
2	0, [Flow], 32, 1, 4
3	0, [Flow], 32, 1, 4
4	1, [2, 3], 64, 4, 1
5	1, [0], 64, 2, 1
6	2, [1, 4, 5], 64, 1, 2
7	2, [4, 5], 64, 8, 2
8	2, [4, 5], 64, 2, 2
9	2, [0, 1, 4, 5], 64, 8, 2
10	3, [0, 1, 5, 6, 9], 128, 4, 2
11	3, [6, 7, 8], 128, 1, 2
12	3, [5, 6, 8, 9], 128, 4, 2
13	3, [4, 5, 6, 8, 9], 128, 8, 2
14	4, [10, 11, 12, 13], 512, 4, 2

A.5 Training details

In our experiments, we use 32 processing units with a total of 64 cores for the training of AssembleNet models and baselines. The memory size is 16GB per core. For the Moments in Time (MiT) dataset training, 8 videos are provided per core: the batch size is 512 with 32 frames per video. The batch size used for Charades is 128 with 128 frames per video. The base framerate we used is 12.5 fps in both datasets. The spatial input resolution is 224x224. We used the standard Momentum Optimizer in TensorFlow with the learning rate of $(0.00625 * \text{batch size})$, 12k warmup iterations, and cosine decay. No dropout is used, and the weight decay is $1e-4$. We used weight decay with $\lambda = 0.0001$ and label smoothing set to 0.2.

Training a model for 10k iterations (during the evolution) took 3~5 hours and fully training the model (for 50k iterations) took ~24 hours per dataset.

We used the TV-L1 optical flow extraction algorithm [32] implemented with tensor operations to obtain flow input.

A.6 Evaluation details

When evaluating a model on the MiT dataset, we provide 36 frames per video. The duration of each MiT video is 3 seconds, making 36 frames roughly correspond to the entire video. For the Charades dataset where each video duration is roughly ~30 seconds, the final class labels are obtained by applying the model to five random 64 frame crops (i.e., segments) of each video. The output multi-class labels are averaged to get the final label, and is compared to the ground truth to measure the average precision scores. The spatial resolution used for the testing is 256x256.